IOP Conf. Series: Journal of Physics: Conf. Series **847** (2017) 012054 doi:10.1088/1742-6596/847/1/012054

Characterization of novel preclinical dose distributions for micro irradiator

J Kodra[1], D Miles[1], S W Yoon[1], D G Kirsch[1] and M Oldham[1]
[1]Dept. of Radiation Oncology, Duke University Medical Center, Durham, NC, USA

Email: jacob.kodra@duke.edu

Abstract. This work explores and demonstrates the feasibility of utilizing new 3D printing techniques to implement advanced micro radiation therapy for pre-clinical small animal studies. 3D printed blocks and compensators were designed and printed from a strong x-ray attenuating material at sub-millimeter resolution. These techniques enable a powerful range of new preclinical treatment capabilities including grid therapy, lattice therapy, and IMRT treatment. At small scales, verification of these treatments is exceptionally challenging, and high resolution 3D dosimetry ($0.5mm^3$) is an essential capability to characterize and verify these capabilities, Here, investigate the 2D and 3D dosimetry of several novel pre-clinical treatments using a combination of EBT film and Presage/optical-CT 3D dosimetry in rodent-morphic dosimeters.

1. Introduction

There is significant current interest in exploring the therapeutic, radiobiological and radio-immunological effects of non-standard radiation dose distributions incorporating high spatial modulation such as GRID and LATTICE therapies [1-3]. Instead of aiming for uniform cell kill throughout the PTV, these treatments aim to reduce toxicity to normal tissue while stimulating by-stander effects, endothelial cell death and immunogenic abscopal effects [4-5] for tumor. The potential for using these treatments to 'prime' the immune response prior to more conventional radiation therapy has also been suggested. In this work we explore and demonstrate the feasibility of implementing IMRT and various highly spatially modulated radiation therapy treatments for a small-animal irradiator using 3D printing techniques to create regular modulated micro-blocks and compensators.

2. Methods

2.1 3D printing of micro-blocks and compensators

A range of 3D printers and printing materials were evaluated. Work presented here used a tungsten-filled polylactic acid (PLA) printing filament (Spool3D, Calgary, Alberta, CA) which was selected for its ease of use and ability to be printed with sub-millimeter resolution, allowing for better quality models. The tungsten within the filament acts as an efficient attenuator at orthovoltage treatment energies. Grid and lattice collimators were created using AutoCad (Autodesk, Inc., San Rafael, CA, USA). The 3D printed collimators used in this study were 5mm thick. IMRT compensators and block shapes were designed from in-house treatment planning software and small animal x-ray CT scans. All collimators, compensators and blocks were printed using an Ultimaker 2+ (Ultimaker,

Geldermalsen, Netherlands) 3D printer. A range of blocks and compensators were created to evaluate the capabilities of the 3D printing of these materials. 3D printer settings depended on the model and the amount of time needed for each print ranged from 15 to 90 minutes.

2.2 Irradiations

All irradiations were performed using the X-RAD 225Cx micro-irradiator (Precision X-ray Inc., North Branford, CT, USA) which has previously been commissioned at our institution [6-7]. Micro-compensators and blocks were mounted onto the end of a standard collimator using a novel in-house adapter (Figure 1). The adaptor enabled precise alignment and convenient replacement of the micro-blocks in a slot tray. All irradiations were performed with the default energy of this device, 225kVp.

Figure 1. Rodent-morphic Presage dosimeter set-up in X-Rad irradiator with radiation grid block mounted to collimator.

2.3 Dosimetry

Dosimetric evaluation of preliminary micro-blocks and compensators was performed through a combination of simple 2D EBT Gafchromic film (Ashland Inc., Covington, KY, USA) irradiations, and high resolution 3D dosimetry in rodent-morphic phantoms using the Presage/optical-CT system [8]. Initial assessment of the attenuation capabilities of the tungsten filament and resolution of the 3D printer, was achieved by placing blocks directly onto a section of EBT2 film and irradiated with an AP field of 2 Gy. EBT2 film was analyzed using an Epson flatbed scanner (Epson America Inc., Long Beach, CA, USA) and an open source image processing software ImageJ (National Institutes of Health, Bethesda, MD, USA).

As a proof of concept, a 3D GRID treatment was designed to deliver 5 Gy to a mouse in 1mm wide bands with 1mm spacing. A 3D printed line grid was mounted to a 40x40mm collimator in the X-Rad, and used to irradiate a custom mouse-shaped Presage dosimeter via a 180-degree arc treatment (Figure 1). High resolution 3D dosimetry [9] was performed using optical-CT readout using established procedures [8, 10, 11]. The optical-CT was set-up to take 1 projection image per degree, for 360 degrees. Using an in-house reconstruction software, the data was reconstructed with 1 mm resolution.

2.4 IMRT

Preliminary testing of implementing IMRT capabilities to the X-Rad have been performed using the IMRTp platform built into CERR (National Institutes of Health, Bethesda, MD, USA) in conjunction with an in-house optimization program. Through this method, fluence maps are generated for the IMRT treatment plan and converted into 3D printed compensators.

3. Results

Radiochromic film readout shows the 3D printed grid and lattice collimators have both high resolution and efficient attenuating capabilities (Figure 2). The films show sharp edges with distinctive alternating regions of low and high dose with average peak-to-peak distance of 2.01 mm, corresponding well with the 1 mm spacing design of the 3D printed grid (Figure 3).

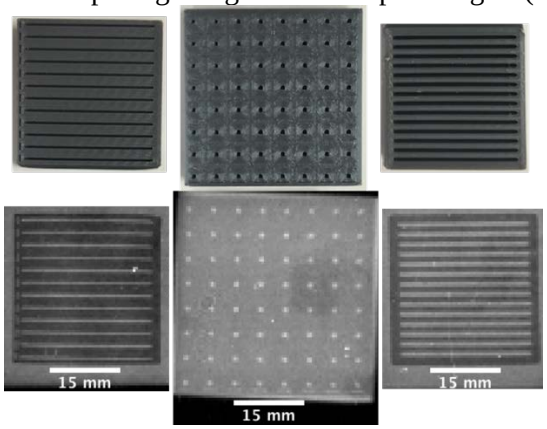

Figure 2. Top row-3D printed collimators of different grid and lattice spacing. Bottom row – corresponding EBT film measurements.

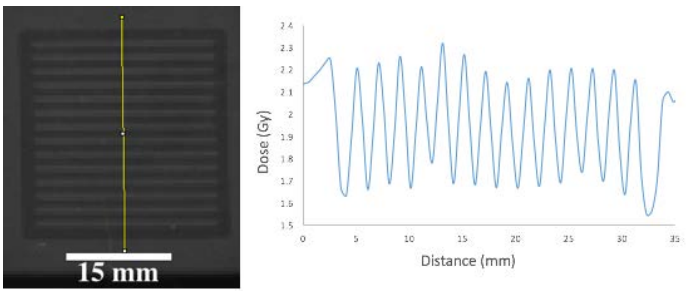

Figure 3. Left-Image an irradiated EBT2 film with grid of 1mm gaps and 1mm spacing. Right-image - Corresponding line profile showing change in optical density (proportional to dose).

Optical-CT readout of the Presage dosimeter shows high change in optical density (OD) for regions unblocked from the radiation beam (Figure 4). Another visualization of this peak-to-valley distribution can be seen in the line profile of the reconstruction (Figure 5).

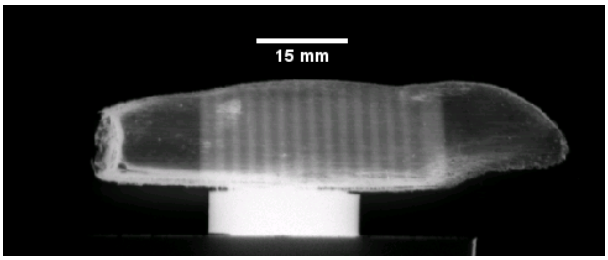

Figure 4. Projection image of PRESAGE rodent-morphic dosimeter treated with 3D printed radiation grid block in place on collimator.

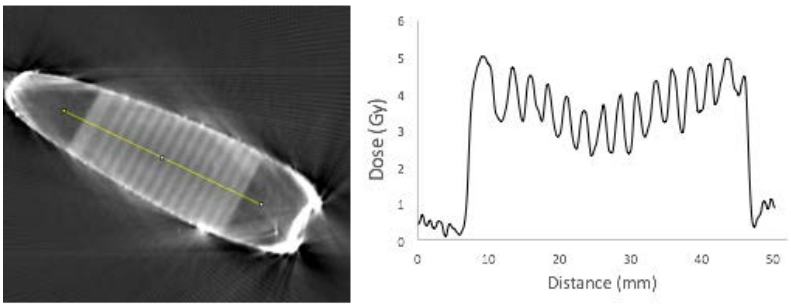

Figure 5. Left image -Reconstruction image of PRESAGE rodent-morphic dosimeter treated with 180-degree grid arc therapy. Right image -Corresponding line profile displaying the peak to valley dose distribution.

Preliminary testing of IMRT compensators show agreement between the generated fluence maps and the irradiated EBT2 film with regions of higher and lower change in OD (Figure 6).

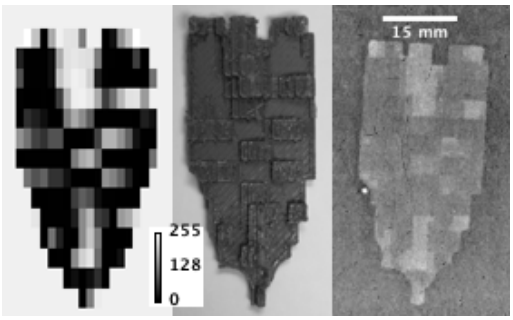

Figure 6. Left- Fluence map generated by in-house program with lighter regions corresponding to lower dose. Center-3D printed compensator of fluence map. Right- scan of an irradiated EBT2 film showing dose distribution with lower dose represented by lighter pixels.

4. Conclusions

Initial testing of 3D printed radiation blocks and compensators for use in small animal radiation therapy studies has shown promising results. A wide variety of spatially fractionated treatments are possible, including micro-IMRT for field sizes up to 4x4cm. Sub-millimeter spatial modulation of dose distribution is feasible with the techniques shown here. Further development work is required to optimize the peak-to-valley differential for GRID and LATTICE treatments. Combinatorial dosimetry approaches (e.g. both film and 3D) are considered essential to cross-validate findings in these extremely challenging dosimetric scenarios.

5. References

[1] Wu X *et al* 2010 *Cureus* **2 e9**
[2] Suarez B *et al* 2015 *Cureus* **7 e389**
[3] Kanagavelu S *et al* 2014 *Radiation Research* **182** 149-62
[4] Formenti S C *et al* 2012 *Int. J. Radiat. Oncol. Biol. Phys.* **84** 879-80
[5] Formenti S C *et al* 2013 *Int. J. Radiat. Oncol. Biol. Phys.* **105** 256-65
[6] Newton J *et al* 2011 *Med. Phys.* **38** 6754-62
[7] Thomas A *et al Med. Phys.* **38** 4846-57
[8] Rankine L J *et al* 2013 *Phys. Med. Biol.* **58** 7791-801
[9] Baldock C *et al* 2010 *Phys. Med. Biol.* **55** R1-63
[10] Bache S T *et al* 2015 *Med. Phys.* **42** 846-55
[11] Cramer C K *et al* 2015 *PloS One* **4**